Available online at www.sciencedirect.com
SCIENCE DIRECT

Remote Sensing of Environment 86 (2003) 150–161

Remote Sensing of Environment

www.elsevier.com/locate/rse

Mapping nonnative plants using hyperspectral imagery

Emma Underwood*, Susan Ustin, Deanne DiPietro

Center for Spatial Technologies and Remote Sensing, University of California, Davis, One Shields Avenue, Davis, CA 95616, USA

Received 12 July 2002; received in revised form 10 February 2003; accepted 22 February 2003

Abstract

Nonnative plant species are causing enormous ecological and environmental impacts from local to global scale. Remote sensing images have had mixed success in providing spatial information on land cover characteristics to land managers that increase effective management of invasions into native habitats. However, there has been limited evaluation of the use of hyperspectral data and processing techniques for mapping specific invasive species based on their spectral characteristics. This research evaluated three different methods of processing hyperspectral imagery: minimum noise fraction (MNF), continuum removal, and band ratio indices for mapping iceplant (*Carpobrotus edulis*) and jubata grass (*Cortaderia jubata*) in California's coastal habitat. Validation with field sampling data showed high mapping accuracies for all methods for identifying presence or absence of iceplant (97%), with the MNF procedure producing the highest accuracy (55%) when the classes were divided into four different densities of iceplant.

Keywords: AVIRIS; Hyperspectral; Invasive plants; Nonnative plants; Iceplant; *Carpobrotus edulis*; Jubata grass; *Cortaderia jubata*; Mapping

1. Introduction

One of the most significant threats to global biodiversity and ecosystem functioning is the spread of invasive plant species (Mooney & Cleland, 2001). Continuing anthropogenic related disturbances, such as land conversion, grazing, and habitat fragmentation, combined with international trade and climate change indicate that these trends are likely to continue (Zedler & Scheid, 1988). In this context, the major challenge for land managers and ecologists is how to effectively manage nonnative plants to preserve native biodiversity. Being able to delineate the spatial extent and to ascertain the severity or intensity of the invasion is essential for resource management (Byers et al., 2002). This information provides a baseline for monitoring future expansion, the effectiveness of control efforts, and assists in identifying targets for control activities such as satellite populations and 'invasion fronts.'

Techniques, such as remote sensing, offer significant opportunities for providing timely information on invasions of nonnative species into native habitats. In contrast to field-based surveys, imagery can be acquired for all habitats, over a much larger spatial area, and in a short period of time. Consequently, researchers have sought to exploit unique phenological, spectral, or structural characteristics of the nonnative species in the image to distinguish them from the mosaic of species around them. To date, there have been two divergent approaches. First, the use of imagery with a high spatial, but low spectral resolution such as black and white or color infrared aerial photographs. Second, the use of digital images with greater spectral resolution although coarser spatial resolution.

Aerial photographs have the benefit of being relatively inexpensive with large amounts of archival data available for many sites and typically have very fine spatial resolution (0.1–2 m). Aerial photography techniques have capitalized on unique visual characteristics at particular times in the focal species' lifecycle. For example, Chinese tamarisk (*Tamarix chinensis*) has been identified using the unique orange-brown color prior to leaf drop (Everitt, Escobar, Alaniz, Davis, & Richerson, 1996), while leafy spurge (*Euphorbia esula*) has distinctive yellow bracts which appear with flowering in late May (Everitt et al., 1995). However, the major disadvantage of this approach is that it relies on the nonnative plant possessing visually

* Corresponding author. Tel.: +1-530-754-6051; fax: +1-530-752-3350.
E-mail address: eunderwoodrussell@ucdavis.edu (E. Underwood).

0034-4257/03/$ - see front matter © 2003 Elsevier Inc. All rights reserved.
doi:10.1016/S0034-4257(03)00096-8

detectable unique characteristics as well as requiring extensive manual labor for processing. Manual tasks include, for example, digitizing and georegistering of imagery as well as time-intensive interpretation requiring both skill and experience (Anderson, Everitt, Richardson, & Escobar, 1993; Everitt et al., 1995). Finally, the resolution of the imagery, along with the associated manual processing time, means that it is only feasible to collect data over a relatively small spatial area.

In contrast, the use of digital multispectral imagery offers the opportunity for automated image processing, access to recent historical data for time series analyses, and large spatial coverage. Some studies have had success even using coarse-resolution (1.1 km pixel) advanced very high resolution radiometer (AVHRR) imagery to identify weeds. For example, Peters, Reed, Eve, and McDaniel (1992) identified moderate to heavy infestations of broom snakeweed (*Gutierrezia sarothrae*) with an average cover > 9% in a 4 × 4 km site. This species was distinguished from grasslands using the normalized difference vegetation index (NDVI) (Tucker, 1979) due to differences in phenological activity. However, successful mapping at this scale has been limited by the coarse resolution and the number of spectral bands (2) of AVHRR. At higher spatial and spectral resolution Landsat 5 thematic mapper (TM) imagery (30 m pixels) was used to predict the distribution of dyers woad (*Isatis tinctoria*) (Dewey, Price, & Ramsey, 1991). Known infestations were mapped and correlated with brightness, greenness, and wetness values derived from the reflectance data. Finally, airborne data acquisition and registration (ADAR) data at 1-m resolution has successfully distinguished different densities of yellow hawkweed (*Hieracium pratense*) invasion using supervised and unsupervised classification techniques (Carson, Lass, & Callihan, 1995). However, the spatial resolutions of TM, like AVHRR imagery, mean that invasive species populations can often only be detected after they become dense and widespread (Carson et al., 1995). In addition, traditional classification techniques, such as isodata

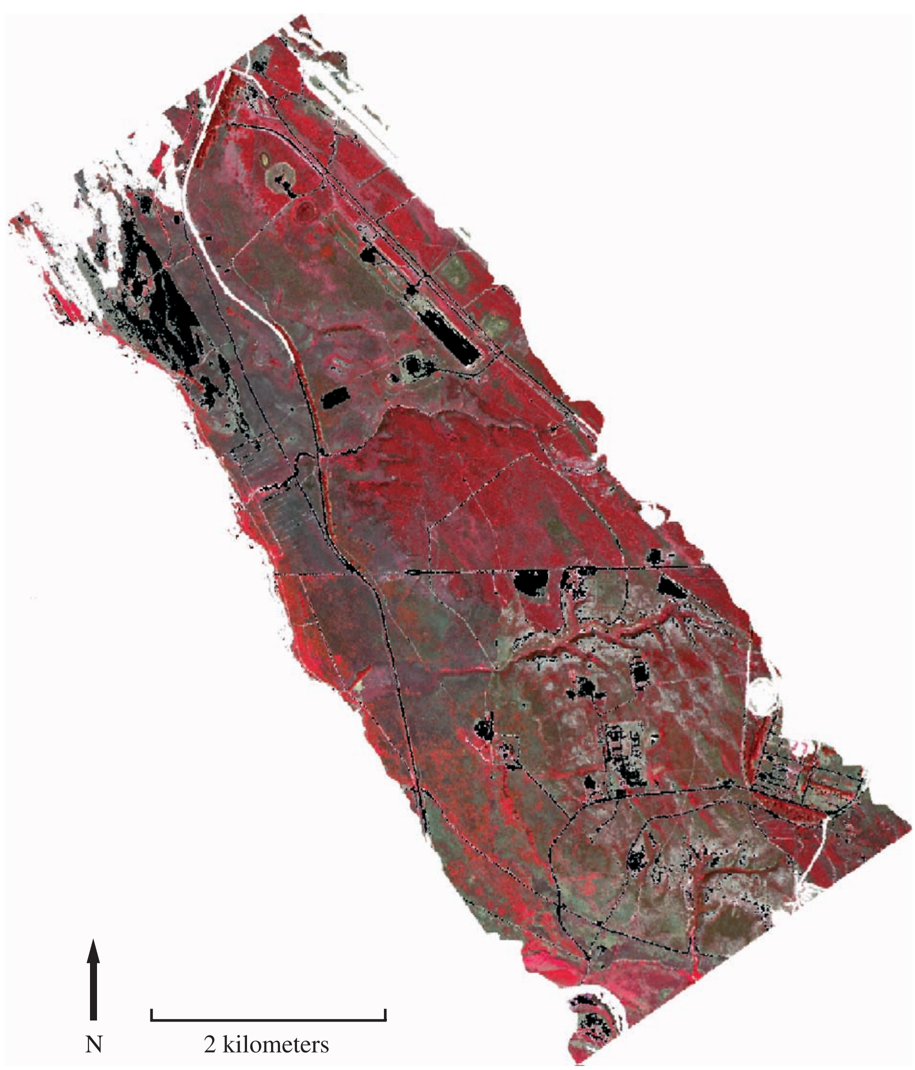

Fig. 1. Color infrared image.

or maximum likelihood, usually identify vulnerable land cover classes, rather than the nonnative species itself; consequently, maps have only a general applicability.

The availability of airborne visible/infrared imaging spectrometer (AVIRIS) imagery with increased spatial and, more critically, fine spectral resolution, offers an enhanced potential for mapping invasive species. Because of the large number of wavebands (224), image processing is able to capitalize on both the biochemical and the structural properties of the target invader. The need for exploring these spectral properties is particularly important when we consider the limitations of using traditionally available wavebands; for example, with color infrared, green vegetation is observed as shades of red. This is seen in Fig. 1, where the majority of land cover appears as 'green vegetation'; thus, identification of individual species, including invasive species, which dominate the coastal margin is impossible, even at 4 m pixel resolutions. However, to date, there has been little evaluation of different processing techniques that take advantage of imaging spectrometry data for identifying invasive plants. The objective of this research is to investigate the use of AVIRIS imagery to detect the invasive species iceplant (*Carpobrotus edulis*) and jubata grass (*Cortaderia jubata*) and, more specifically, to compare three techniques for processing the imagery: minimum noise fraction (MNF), continuum removal, and band ratio indices.

The minimum noise fraction is a linear transformation that consists of two separate principle component analysis (PCA) rotations, separating noise from signal and compressing spectral information to a few bands (Green, Berman, Switzer, & Craig, 1988). As a standard image-processing technique, we are interested in assessing how well it performs for identifying our focal species. Band ratio indices create new spectral bands which are useful for emphasizing certain physiologically important features. For example, NDVI has been used for mapping green vegetation, while at the leaf and the stand scales the red/green ratio and water band indices have been used to describe relative levels of anthocyanin and water, respectively (Peñuelas, Pinol, Ogaya, & Filella, 1997; Gamon & Surfus, 1999). In this study we investigate whether vegetation indices can capture the characteristics of a specific species within a mosaic of other vegetation. Finally, we seek to assess the potential of simply using an analysis of the water absorption bands to map weeds. The continuum removal technique isolates spectral features and standardizes reflectance across the liquid water absorption features so that they may be intercompared (Clark & Roush, 1984). The advantage is that values are independent of differences across the image such as illumination or shadow. These three processes were compared for their ability to delineate the spatial extent and the density of iceplant and jubata grass and also to critically evaluate the relative ease of processing and repeatability of each method.

2. Methods

2.1. Study site and vegetation descriptions

The study site for this research is Vandenberg Air Force Base (VAFB) located along the central coast of California (Fig. 2). VAFB is 39,800 ha and is used primarily for developing and testing missiles and satellite launches for the Department of Defense and National Aeronautics and Space Administration (NASA). Consequently, significantly large intact blocks of land remain in one of the last undeveloped open areas of coastal California (Keil & Holland, 1998). There are 836 vascular plants documented at VAFB, however, almost a quarter are invasive species. In particular, *C. edulis* and *C. jubata* have successfully invaded two native community types: coastal dune scrub community and maritime chaparral (Keil & Holland, 1998). The coastal scrub community forms a relatively continuous cover of low to medium shrubs (< 1 m tall), subshrubs, and herbs (Keil & Holland, 1998) and is dominated by California sagebrush (*Artemisia californica*), coyote bush (*Baccharis pilularis*), and mock heather (*Ericameria ericoides*) (Table 1). It is one of the most threatened community types in California, being rapidly fragmented and replaced by suburban developments, which makes the extensive iceplant invasion into remaining habitats of particular concern. The second community that iceplant is encroaching on is the maritime chaparral community characterized by broad-leafed and needle-leafed sclerophyllous shrubs such as manzanita (*Arctostaphylos purissima*, *Arctostaphylos rudis*) and chamise chaparral (*Adenostoma fasciculatum*) (Table 1). An extensive area of this community—the Burton Mesa chaparral—is noted as one of the rarest and most threatened chaparral types in California, harboring extraordinary biodiversity (The Nature Conservancy, 1991). Invading iceplant, jubata grass, and other invasive species, such as veldt grass (*Ehrharta caly-*

Fig. 2. Locator map: Vandenberg Air Force Base.

Table 1
Community types used for Regions of Interest at VAFB (based on Keil & Holland, 1998)

Community type	Species (Latin)	Species (common name)
(1) Intact coastal dune scrub	*Artemisa californica*	California sagebrush
	Baccharis pilularis	Coyote bush
	Croton californicus	Croton
	Ericameria ericoides	Mock heather
	Eriogonum parvifolium	Coastal buckwheat
	Lotus scoparius	Deerweed
	Lupinus arboreus	Tree lupine
	Lupinus chamissonis	Silver lupine
	Senecio Blochmaniae	Blochman's groundsel
(2) Intact maritime chaparral	*Arctostaphylos rudis*	Shag bark manzanita
	Arctostaphylos purissima	La Purisima manzanita
	Ceanothus impressus	Mountain haze
	Mimulus aurantiacus	Monkey flower
	Adenostoma fasciculaturm	Chamise
	Horkelia cuneata	Horkelia
(3) Iceplant invaded coastal scrub	Type 1 with *Carpobrotus edulis*	Iceplant
(4) Iceplant invaded chaparral	Type 2 with *Carpobrotus edulis*	Iceplant
(5) Jubata invaded chaparral	Type 2 with *Cordateria jubata*	Jubata grass

cina), form mosaics with the native species. The focus of this research is the encroachment of iceplant and jubata grass into these native communities and specifically on the ability of AVIRIS to identify pixels of different densities of these species, the premise being that lower densities at the margins of the distribution represent invasion fronts and, thus, critical areas for management attention.

Iceplant, also known as the Hottentot fig (Fig. 3), is native to South Africa and was introduced into California in ballast sand; by the 1950s, it was used extensively for stabilizing land adjacent to roads. *C. edulis* is a succulent perennial (Albert, 1995) forming mats up to 20 m wide and 50 cm deep (D'Antonio, 1993). The species' success is due to its tolerance of a range of soil moisture and nutrient conditions, and utilizing a number of mammals for seed dispersal (D'Antonio, 1993). Ecological impacts of iceplant include aggressive competition with native species, such as Tidestrom's lupine (*Lupinus tidestromii*), destabilizing native dune communities and modifying soil pH (Moss, 1990). Economic impacts stem from time and financial costs associated with both manual and mechanical controls.

The other invasive species of concern at VAFB is jubata grass (*C. jubata*), a perennial tussock grass from the Andes Mountains, characterized by huge creamy-pink plumes and long leaves (Fig. 4). Introduced as an ornamental species, it now dominates much of the coastal habitat from central California to southern Oregon (Lambrinos, 2001).

Jubata grass poses a significant threat to Mediterranean ecosystems because of its prolific wind dispersed seeds, tolerance of a broad range of habitats, and its competitiveness for light, moisture, and nutrients (Cowan, 1976).

2.2. Description of fieldwork and global positioning system (GPS) data collection

Existing geographic information system (GIS) data layers were acquired from VAFB including topographic

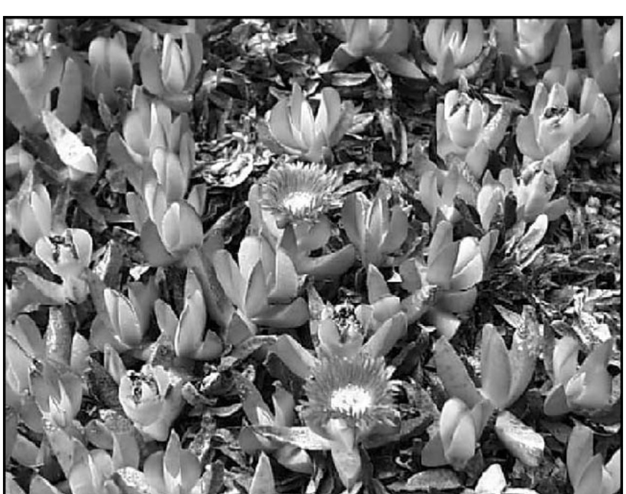

Fig. 3. Iceplant (*Carpobrotus edulis*).

Fig. 4. Jubata grass (*Cortaderia jubata*).

maps, vegetation maps, road layers, land use history, which were converted into a common Universal Transverse Mercator (Zone 10 north, datum Nad27) projection. A field sampling methodology was designed and implemented in summer 2000 to coincide with the acquisition of the AVIRIS imagery. Sampling was undertaken in five community types identified a priori: intact coastal dune scrub, intact maritime chaparral, iceplant invaded scrub, iceplant invaded chaparral, and chaparral invaded by jubata grass. Post-collection analysis confirmed that these communities varied significantly in their species composition (richness and diversity) and vegetation characteristics (structure). The location of the 352 fieldwork plots was random, but consideration was given to ease of access and location within the flightline. Field data were collected at three different scales to provide information from the plot through to the community level: measurements included percent cover by species, species height, type and size of disturbances, and soil characteristics. GPS readings (Trimble Pro-XRS, Trimble Navigation) were taken of plot centers and around pure polygons of iceplant, jubata grass, and intact community types. Fieldwork also involved the acquisition of field-based reflectance spectra of the dominant native and nonnative plant species and soil types in the area. Data were acquired at the time of the overflights using a GER 2500 (Geophysical Research) field-portable spectrometer (400–2500 nm). Owing to almost continual coastal fog during the period around the overflight, only 80 individual spectra of target species at VAFB were acquired. AVIRIS data were acquired by the NOAA Twin Otter aircraft on September 9, 2000 at 3810 m, providing a nominal pixel resolution of 4.5 m.

2.3. Data-processing techniques

The imagery was atmospherically corrected from radiance to reflectance with ACORN (Analytical Imaging and Geophysics LLC v.4), a commercial package based on MODTRAN, using the reflectance of target features from spectrometer data acquired in the field. The AVIRIS scenes were spectrally and spatially subsetted to allow for rapid georeferencing and to remove bands containing a high degree of noise (ENVI software v.3.4; Research Systems). Noise refers to bands where there is a high degree of speckle or banding, and missing data. Wavebands 1–4 (374–404 nm), 103–120 (1314–1484 nm), 148–179 (1763–2061 nm), and 220–224 (2469–2509 nm) were removed based on visual inspection of each band of the imagery. Masks were created to limit processing to vegetated areas, identified as pixels with an NDVI > 0.2, to reduce the number of classes in the classification process. In addition to the 352 field plots, an independent set of GPS regions of interest (ROIs) of known community types and species were acquired, differentially corrected (Pathfinder Office v.2.8; Trimble Navigation), and used as inputs into the supervised classifications.

A supervised maximum likelihood classification was performed on the results of each of the three processing techniques (MNF, continuum removal, and band ratio indices). Eight intact and invaded community classes were generated, comprised of the five community types identified for fieldwork (intact scrub, intact chaparral, scrub invaded by iceplant, chaparral invaded by iceplant, and chaparral invaded by jubata grass). In addition, we also classified different densities of iceplant within the scrub habitat—less than 50%, 51–75%, 76 – 90%, and 91–100%—to assess of how well the different techniques could distinguish mosaics within single community type. No smoothing or merging of classes was performed to improve the spatial distribution of clusters.

2.3.1. Minimum noise fraction classification

A minimum noise fraction (MNF) was performed on each flightline to reduce and compress the data and to increase the speed of data processing. The MNF sequentially performs two principle component analyses (PCA) on the data: the first separates white noise (i.e., uninformative data), and the second recombines these bands into new composite bands which account for most of the variance in the original data (informative data). Based on the MNF

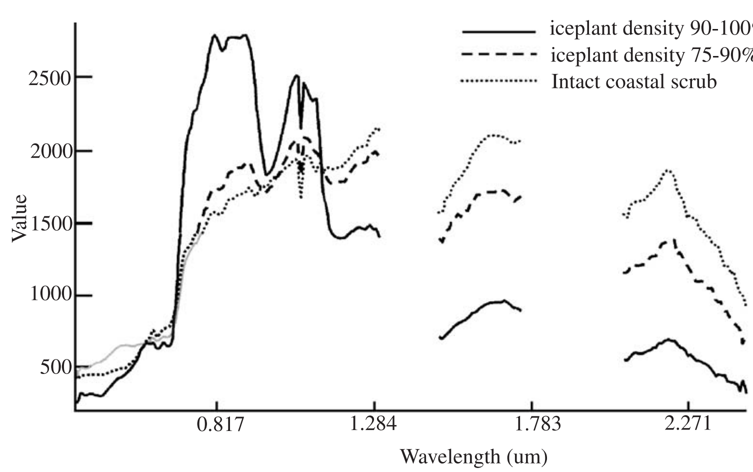

Fig. 5. Reflectance spectra showing absorption in the water band.

Table 2
Wavebands used to calculate vegetation indices (adapted from Fuentes, Gamon, Qiu, Sims, & Roberts, 2001)

Index	Bands	Wavelengths	Source
Red/green ratio	Chlorophyll	683/510	Gamon and Surfus (1999)
Index of pigment	Pigment	750/710	Gamon and Surfus (1999)
Index of water 1	Water content	970/900	Peñuelas et al. (1997)
Index of water 2	Water content	1193/1126	Image inspection
NDVI	Green vegetation	895 − 675/ 895 + 675	Modified from Tucker (1979)

output graph of eigenvectors and by visually inspecting the new bands, a conservative noise floor was established and the first 12 bands were selected as inputs for the classification. The results of the MNF were georegistered and a maximum likelihood classification was performed.

2.3.2. Continuum removal for water bands

The second technique used to classify iceplant was a continuum removal of the water absorption bands, which was assumed to be particularly sensitive to the fleshy succulent leaves of *C. edulis* (Fig. 5). Continuum removal standardizes reflectance spectra to allow for comparison of absorption features. The process involved spectrally subsetting 33 bands of the image: 15 around 985 nm (between the wavelengths 924–1061 nm) and 18 around 1184 nm (1108–1254 nm). Water absorption was calculated from the area under the absorption feature divided by the area under the continuum, resulting in a single band ranging in values from 0 to 1; the lower the value, the greater the absorption. This is illustrated in Fig. 5, which shows a comparison of the

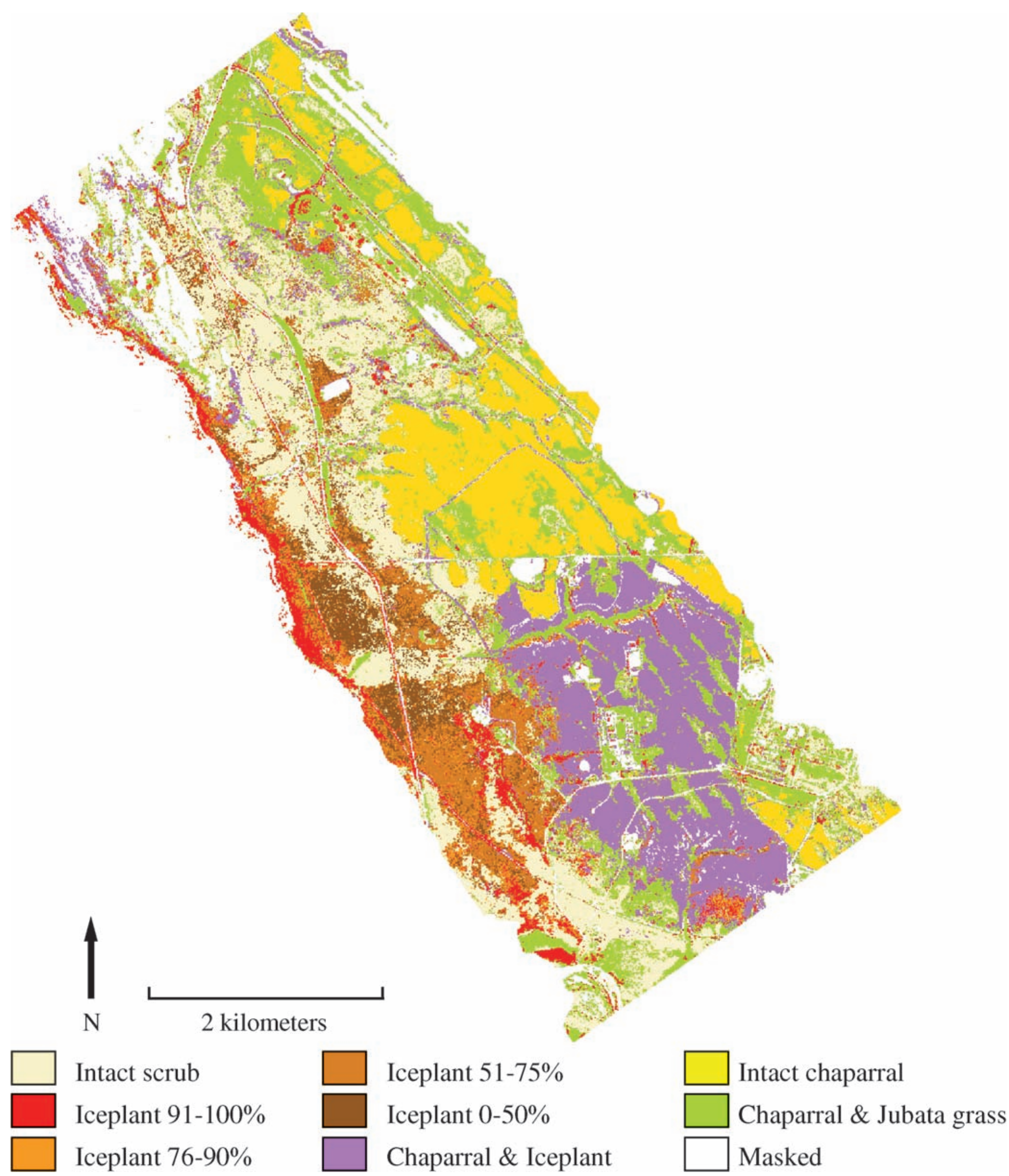

Fig. 6. Results of supervised classification of MNF results.

reflectance spectra of pixels having two different densities of iceplant compared to a pixel of intact coastal scrub. The graph shows two distinctive absorptions for dense iceplant centered on 985 nm and 1184 nm wavelengths. Visual inspection of the resulting images showed greater accuracy when using wavelengths centered around 985 nm than the 1184 nm feature due to the background atmospheric water vapor absorption at 1240 nm. A maximum likelihood classification was performed on these results.

2.3.3. Band ratio indices

We explored the use of selected vegetation indices to use in the classification, which emphasize the biochemical and the biophysical properties of the vegetation contained in physiologically important bands. Vegetation indices are clearly linked with foliage chlorophyll absorption (Ustin, Smith, Jacquemoud, Verstraete, & Govaerts, 1999); however, such indices have also been correlated with Leaf Area Index (LAI) (Qi, Cabot, Moran, & Dedieu, 1995), percent green cover and biomass (Gamon et al., 1995), productivity (Weigand & Richardson, 1987), and photosynthetic capacity (Sellers, 1985). The NDVI is perhaps the most well known of these vegetation indices (Curran, 1989; Tucker, 1979); however, the water band index has been shown to be a good indicator of leaf and canopy water content (Peñuelas, Pinol, Ogaya, & Filella, 1997; Serrano, Ustin, Roberts, Gamon, & Peñuelas, 2000) and the red-edge spectral parameters for chlorophyll concentration (Miller, Hare, & Wu, 1990; Zarco-Tejada & Miller, 1999). Even so, using a combination of vegetation indices for a classification has received limited application for ecological studies (Fuentes, Gamon, Qiu, Sims, & Roberts,

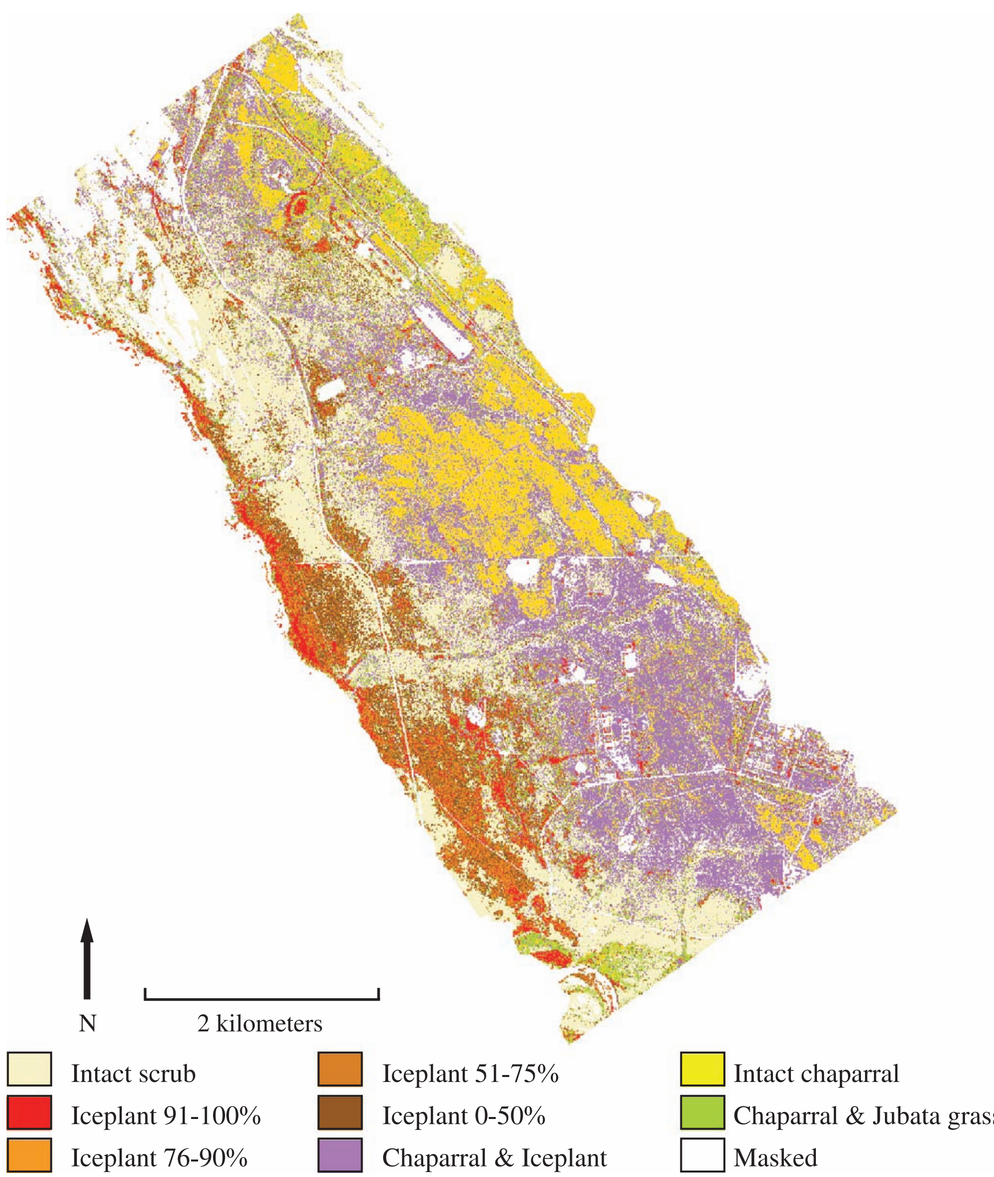

Fig. 7. Results of unsupervised classification of continuum removal results.

2001). We seek to assess how well a land cover classification based on data from this technique compares to the results using MNF and continuum removal approaches. Five indices were calculated on the calibrated image, capturing NDVI, water absorption, greenness, and pigment properties (Table 2), and combined into a single image. The eight different community classes were subsequently generated using the maximum likelihood classifier.

3. Results

A visual comparison of the three classification results (Figs. 6–8) shows that iceplant is clearly distinguished in all analyses with a similar spatial configuration: highest densities parallel to the coastline and tapering off with increasing distance inland (in a northeast direction). Separation of different density levels of iceplant is evident in all three images. Field validation was undertaken in August 2001 to obtain ocular cover estimates by species of the classification performance and to identify areas of misclassification.

An accuracy assessment of the classification results was performed using 277 of the 352 plot centers acquired in the five community types, located over a 7 × 3 km swath of the flightline. Analysis of field data revealed that in the invaded scrub community, the mean cover of iceplant was 43% and 13% in the invaded chaparral community, whereas jubata grass had a 27% mean cover in the invaded chaparral community type (Ustin & Moser, 2002). For the purpose of the accuracy assessment, the four iceplant density classes were combined into one. The average number of points for each community was 55, which is in accordance with the

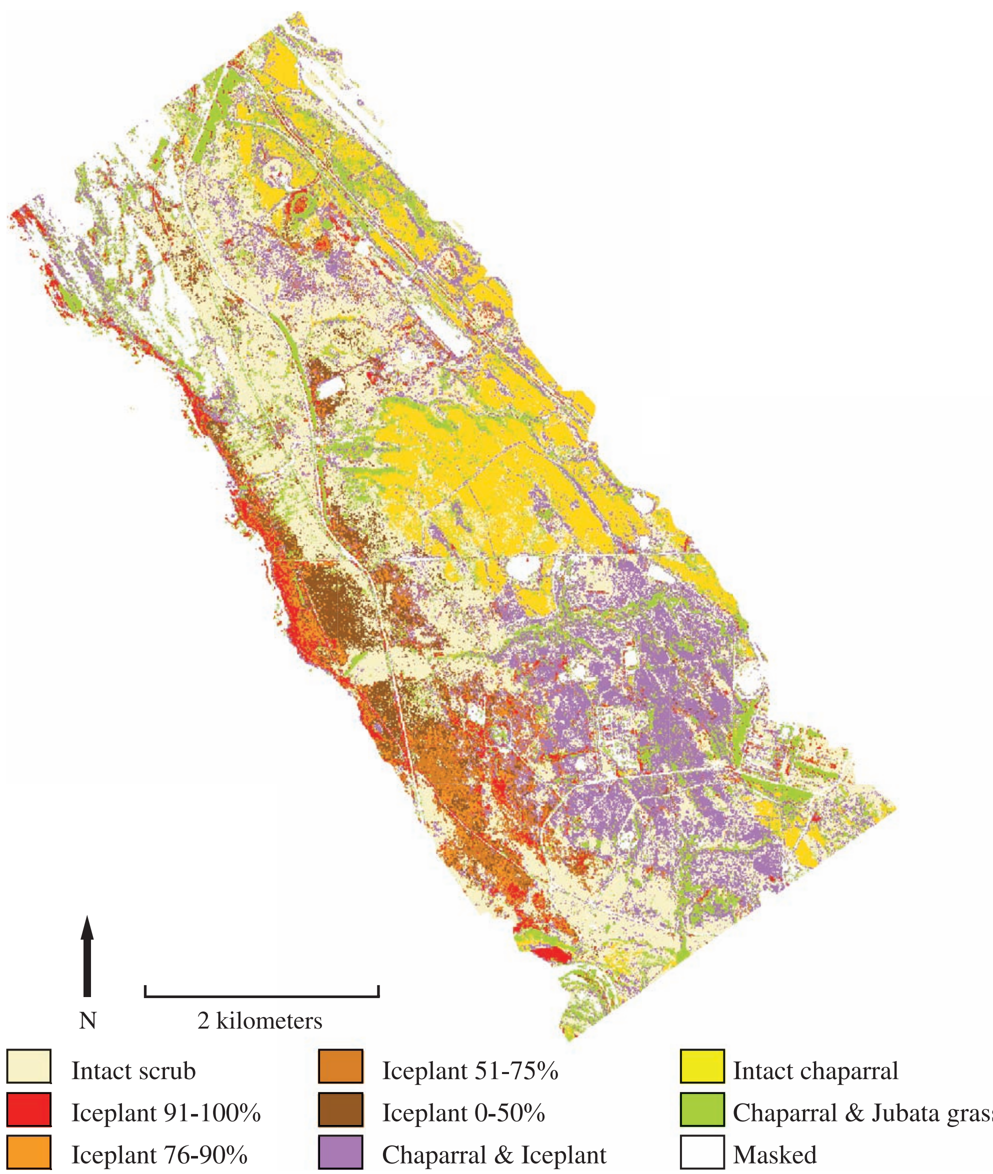

Fig. 8. Results of supervised classification of band ratios results.

Table 3
Confusion matrix for classification on MNF image (ground validation pixels)

Class	scrub_intact	scrub_ice	chap_intact	chap_ice	chap_pamp	Total
Unclassified	0	5	0	0	1	6
scrub_intact	45	14	2	0	9	70
scrub_ice	7	49	0	2	1	59
chap_intact	0	0	25	0	4	29
chap_ice	0	0	11	45	1	57
chap_pamp	3	0	5	1	47	56
Total	55	68	43	48	63	277

Class	Prod. acc (%)	User acc. (%)
scrub_intact	81.82	64.29
scrub_ice	72.06	83.05
chap_intact	58.14	86.21
chap_ice	93.75	78.95
chap_pamp	74.60	83.93

Overall accuracy = 76.17%; kappa coefficient = 0.70.

Table 4
Confusion matrix for classification on continuum removal image (ground validation pixels)

Class	scrub_intact	scrub_ice	chap_intact	chap_ice	chap_pamp	Total
Unclassified	0	5	0	0	1	6
scrub_intact	40	12	3	3	12	70
scrub_ice	2	47	2	1	1	53
chap_intact	0	0	17	1	16	34
chap_ice	7	2	16	36	21	82
chap_pamp	6	2	5	7	12	32
Total	55	68	43	48	63	277

Class	Prod. acc (%)	User acc. (%)
scrub_intact	72.73	57.14
scrub_ice	69.12	88.86
chap_intact	39.53	50
chap_ice	75	43.9
chap_pamp	19.05	37.5

Overall accuracy = 54.87%; kappa coefficient = 0.44.

Table 5
Confusion matrix for classification on band ratio image (ground validation pixels)

Class	scrub_intact	scrub_ice	chap_intact	chap_ice	chap_pamp	Total
Unclassified	0	5	0	0	1	6
scrub_intact	50	14	6	9	23	102
scrub_ice	1	46	0	1	1	49
chap_intact	0	0	23	1	16	40
chap_ice	1	0	9	33	11	54
chap_pamp	3	3	5	4	11	26
Total	55	68	43	48	63	277

Class	Prod. acc (%)	User acc. (%)
scrub_intact	90.91	49.02
scrub_ice	67.65	93.88
chap_intact	53.49	57.5
chap_ice	68.75	61.11
chap_pamp	17.46	42.31

Overall accuracy = 58.84%; kappa coefficient = 0.49.

suggested 50 verification points per class (Jensen, 1996). A comparison between the classified image and the validation ROIs was generated through standard postclassification techniques in ENVI software, using a confusion matrix (Congalton, 1991, Jensen, 1996). The confusion matrices (Tables 3–5) include the overall accuracy (total number of ground validation pixels classified correctly/total number of pixels) and the kappa coefficient, which expresses the proportionate reduction in error achieved by a classifier as compared with the error of a completely random classifier (Lillesand & Kiefer, 1994).

A comparison of the overall accuracy results shows that the supervised classification of the MNF results performed best, 76.2% (kappa = 0.70), compared to 54.9% (kappa = 0.44) for the continuum removal classification, and 58.8% (kappa = 0.49) for the band ratio technique.

However, perhaps what is more informative, given the management focus for detecting invasions of iceplant and jubata grass into adjacent habitats, is the users' accuracy. The users' accuracy is calculated as the ratio of the number of reference points that are correctly classified divided by the total number of reference points mapped as that class. As such, it is a measure of the percentage of area within a class that is mapped correctly. In contrast to the overall accuracy, the users' accuracy of the MNF was the lowest, 83%, compared to 94% and 89% for the band ratios and continuum removal, respectively. This implies that while the MNF is able to produce a more accurate map of multiple vegetation classes, the continuum removal and the band ratio techniques are better suited for detecting species with distinct characteristics, such as iceplant, with its distinctive succulent characteristics.

Although these results for detecting scrub invaded by iceplant are relatively high, in part attributable to the characteristics of the species, other results emphasize the importance of the adjacent species with which it forms mosaics. For example, the users' accuracy for chaparral invaded by iceplant shows that the MNF approach performs better (79%), with the continuum removal (44%) and the band ratios (61%) performing worse. This suggests that the chaparral species are masking the detection of iceplant, e.g., when it is overgrown and concealed by taller species in the canopy such as the chamise and manzanita shrubs.

Interestingly, if we assess the ability of the three techniques to classify the other invaded community type (jubata invaded chaparral), the users' accuracy for the MNF is comparable to that for the iceplant (84%); however, the performance of the continuum removal (38%) and the band ratios (42%) is much poorer, which helps explain the lower overall accuracy of these classifications.

4. Discussion

Effective management of invasive species requires accurate knowledge of their spatial distribution and density, which are captured to different degrees by the processing methods. The following discussion evaluates the three approaches in terms of accuracy, logistics of processing, and ease of interpretation, which are all necessary considerations for management.

The confusion matrices demonstrate that the MNF performed best for classifying all five vegetation communities within the flightline; however, in terms of classifying one of the target species, iceplant, the continuum removal and the band ratio methods actually performed better. The MNF technique was most capable of distinguishing a range of community types because it uses significantly more information from the image; the classification utilized the 12 most informative transformed bands. In contrast, the band ratio technique uses five key indices which are able to capitalize on the physiological properties of iceplant (94% accuracy), but are less savvy at distinguishing different vegetation communities. Likewise, the continuum removal method relies solely on the 15 bands around the 985 nm water absorption feature, which explains why it performed extremely well for classifying areas of iceplant, but, again, poorly for classifying a range of communities.

One disadvantage of the continuum removal classification is that it produced a very speckled image with single and double pixels scattered throughout. Even after a sieving and clumping was performed to generalize the spatial patterns in the image, the overall accuracy only increased by 3% and the kappa only marginally (0.44 to 0.48). This improvement in accuracy is not significant and not warranted at the expense of losing information, particularly along critical invasion fronts. Other problems that need to be recognized are the potential sources of error in the classifiers which is attributable to both the accuracy of the image georegistration and the GPS points, despite differentially correcting the acquired positions.

Interpretation of the different techniques varied markedly. The MNF method was the most difficult to interpret. Although values from each of the eigenvectors generated by the PCA can be graphed, interpreting the basis of spectral variation was difficult. Even in wavelengths of water absorption, there were no consistently high eigenvalues. Alternatively, using the band ratios has the advantage of being more intuitive, highlighting ecophysiological information about the vegetation that can be readily related to the data collected in fieldwork.

From a processing perspective, the continuum removal method was by far the most efficient, which involved running a single standard procedure in the ENVI software. In contrast, the MNF procedure was time- and processing-intensive, taking several hours to run and creating a 1.8 GB file for each of the two processing modes. In terms of identifying repeatable methods for future use, the continuum removal and the band ratio techniques are easily transportable for images acquired at different times or over different geographic areas. In contrast, the MNF approach cannot be applied to new data as it is unique to the variance of each flightline.

In brief, the continuum removal method is a reliable method for depicting presence/absence of iceplant within a scrub community. Coupled with this is the ease and efficiency of processing, which makes it an attractive approach for inexperienced users of hyperspectral data. Such a method is also likely to be applicable to other invasives such as the giant reed (*Arundo donax*), which has a high water content in the stem. Band ratios have also proved to be adequate, if the indices used are able to capitalize on pertinent characteristics of the target species. In contrast, the MNF approach is most suitable for delineating entire community types. The choice of the particular approach largely rests on the management objectives, e.g., whether to map three invaded community types across the flightline or to focus on detecting the invasion front of one target species as it encroaches into the adjacent native scrub community. The latter could be argued as more important if the key concern is prioritizing control of new infestations.

Land managers wishing to use imagery for mapping and monitoring invasive plants have a tradeoff between spatial and spectral resolutions and costs. At one extreme, the virtues of low spectral, high spatial resolution imagery (aerial photos) are well known (see Section 1), while this research illustrates that AVIRIS imagery offers improved opportunities for mapping invasive plants in a matrix of other vegetation types. The improved spectral resolution of the AVIRIS imagery permits identification of vegetation characteristics that are not possible using multispectral wavebands traditionally used in remotely sensed imagery (Fig. 1). However, one interesting question is whether further improvements in resolutions are necessary. Interestingly, we found for one of the target species, iceplant, that it was possible to achieve successful results using only a portion of wavebands available (band ratios and continuum removal), which could potentially mean fewer bands need to be acquired and processed, with possibly lower associated costs. However, the specific bands needed to map the full range of land cover types may still require a hyperspectral imager. Similarly, the 4 m resolution of the AVIRIS data also proved sufficient for detecting *C. edulis* and *C. jubata*. Despite the common belief that higher spatial resolutions are necessarily better, in this case, it might have produced only marginally improved results, but disproportionately increased the computing and processing requirements. Although the current costs of hyperspectral data means that frequent acquisitions over large areas are probably not feasible, it is a highly appropriate technique for monitoring hotspots of invasions along selected transects. In addition, various data nesting strategies might be employed to optimize the spatial and spectral resolutions required.

The results produced by this image processing can also provide the foundation for predictive modeling of invasive species distributions. Rule-based models can be developed using pixels classified as harboring the target species, together with selected plot data from fieldwork, GIS-derived data layers, and additional variables gleaned from the hyperspectral imagery.

5. Conclusion

This research describes encouraging findings for using hyperspectral imagery to map iceplant and jubata grass in California's Mediterranean-type ecosystems. Given the ecological and economic impacts of invasive plants, together with their rates of spread, they constitute one of the most critical issues for many land managers (Goodall & Naude, 1998). The immediate benefit of this research has been to contribute to the knowledge base of land managers at VAFB by providing improved information on the spatial extent and the density of the iceplant and jubata grass, which will lead to better protection of the native biodiversity. Additionally, the project evaluated three different methods for processing AVIRIS imagery. The next step is to evaluate how well these approaches can be applied to invasions of these species in different habitat types and also their ability to detect other invasive species.

Acknowledgements

We would like to thank John Brooks, Amparo Rifa, and George Scheer for helping to conduct fieldwork. Also, we thank George Scheer, Pablo Zarco-Tejada, and Karen Olmstead from CSTARS at U.C. Davis for assistance in processing of the imagery. We also thank Teresa Magee at Dynamac for providing input advice on the project. Finally, we are grateful to Pablo Zarco-Tejada from CSTARS for helpful comments in reviewing the paper and the TNC Wildland Invasive Species Team for providing Fig. 4. Funding for this research was provided by the Strategic Environmental Research and Development Program and NSF's IGERT program.

References

Albert, M. E. (1995, Spring). Portrait of an Invader II: The ecology and management of *Carpobrotus edulis*. *CalEPPC News,* 4–6.

Anderson, G. L., Everitt, J. H., Richardson, A. J., & Escobar, D. E. (1993). Using satellite data to map false broomweed (*Ericameria austrotexana*) infestations on south Texas rangelands. *Weed Technology*, *7*, 865–871.

Byers, J. E., Reichard, S. H., Randall, J. M., Parker, I. M., Smith, C. S., Lonsdale, W. M., Atkinson, I. A. E., Seastedt, T. R., Williamson, M., Chornesky, E., & Hayes, D. (2002). Directing research to reduce the impacts of nonindigenous species. *Conservation Biology, 16*(3), 630–640.

Carson, H. W., Lass, L. W., & Callihan, R. H. (1995). Detection of yellow hawkweed with high resolution multispectral digital imagery. *Weed Technology*, *9*, 477–483.

Clark, R. N., & Roush, T. L. (1984). Reflectance spectroscopy: Quantitative analysis techniques for remote sensing applications. *Journal of Geophysical Research*, *89*, 6329–6340.

Congalton, R. G. (1991). A review of assessing the accuracy of classifications of remotely sensed data. *Remote Sensing of Environment*, *37*, 35–46.

Cowan, B. (1976). The menace of pampas grass. *Fremontia*, *4*(2), 14–16.

Curran, P. J. (1989). Remote sensing of foliar chemistry. *Remote Sensing of Environment*, *30*, 271–278.

D'Antonio, C. (1993). Mechanisms controlling invasion of coastal plant communities by the alien succulent *Carpobrotus edulis*. *Ecology*, *74*(1), 83–95.

Dewey, S. A., Price, K. P., & Ramsey, D. (1991). Satellite remote sensing to predict potential distribution of dyers woad (*Isatis tinctoria*). *Weed Technology*, *5*, 479–484.

Everitt, J. H., Anderson, G. L., Escobar, D. E., Davis, M. R., Spencer, N. R., & Andrascik, R. J. (1995). Use of remote sensing for detecting and mapping leafy spurge (*Euphorbia esula*). *Weed Technology*, *9*, 599–609.

Everitt, J. H., Escobar, D. E., Alaniz, M. A., Davis, M. R., & Richerson, J. V. (1996). Using spatial information technologies to map Chinese tamarisk (*Tamarix chinensis*) infestations. *Weed Science*, *44*, 194–201.

Fuentes, D. A., Gamon, J. A., Qiu, H. L., Sims, D. A., & Roberts, D. A. (2001). Mapping Canadian boreal forest vegetation using pigment and water absorption features derived from the AVIRIS sensor. *Journal of Geophysical Research-Atmospheres*, *106*(D24), 33565–33577.

Gamon, J. A., & Surfus, J. S. (1999). Assessing leaf pigment content and activity with a reflectometer. *New Phytologist*, *143*(1), 105–117.

Gamon, J. A., Field, C. B., Goulden, K. L., Griffin, A. E., Hartley, G., Joel, G., Peñuelas, J., & Vallentini, R. (1995). Relationships between NDVI, canopy structure, and photosynthesis in three Californian vegetation types. *Ecological Applications*, *4*, 28–41.

Goodall, J. M., & Naude, D. C. (1998). An ecosystem approach for planning sustainable management of environmental weeds in South Africa. *Agriculture Ecosystems and Environment*, *68*, 109–123.

Green, A. A., Berman, M., Switzer, P., & Craig, M. D. (1988). A transformation for ordering multispectral data in terms of image quality with implications for noise removal. *IEEE Transactions on Geoscience and Remote Sensing*, *26*, 65–74.

Jensen, J. R. (1996). *Introductory digital image processing. A remote sensing perspective* (pp. 247–249). New Jersey: Prentice Hall.

Keil, D. J., & Holland, V. L. (1998). The vegetation of Vandenberg Air Force Base. Report prepared for The Nature Conservancy and Vandenberg Air Force Base.

Lambrinos, J. G. (2001). The expansion history of a sexual and asexual species of *Cortaderia* in California, USA. *Journal of Ecology*, *89*(1), 88–98.

Lillesand, T. M., & Kiefer, R. W. (1994). *Remote sensing and image interpretation*. New York: Wiley.

Miller, J. R., Hare, E. W., & Wu, J. (1990). Quantitative characterization of the vegetation red edge reflectance: 1. An inverted-Gaussian reflectance model. *International Journal of Remote Sensing*, *11*(10), 1755–1773.

Mooney, H. A., & Cleland, E. E. (2001). The evolutionary impact of invasive species. *Procedures of National Academy of Science*, *98*(10), 5446–5451.

Moss, T. K. (1990). Ice Plant eradication and native landscape restoration. *Asilomar State Park Newsletter,* 155–156.

Peñuelas, J., Pinol, J., Ogaya, R., & Filella, I. (1997). Estimation of plant water concentration by the reflectance Water Index WI (R900/R970). *International Journal of Remote Sensing*, *18*(13), 2869–2875.

Peters, A. J., Reed, B. C., Eve, M. D., & McDaniel, K. C. (1992). Remote sensing of broom snakeweed (*Gutierrezia sarothrae*) with NOAA-10 spectral image processing. *Weed Technology*, *6*, 1015–1020.

Qi, J., Cabot, F., Moran, M. S., & Dedieu, G. (1995). Biophysical parameter estimations using multidirectional spectral measurements. *Remote Sensing of Environment*, *54*, 71–83.

Sellers, P. J. (1985). Canopy reflectance, photosynthesis and transpiration. *International Journal of Remote Sensing*, *6*, 1335–1372.

Serrano, L., Ustin, S. L., Roberts, D. A., Gamon, J. A., & Peñuelas, J. (2000). Deriving water content of chaparral vegetation from AVIRIS data. *Remote Sensing of Environment*, *74*(3), 570–581.

TNC (1991). Fish and wildlife management plan for Vandenberg Air Force Base. Revision Number 3 for Plan Period August 1991 to August 1996. The Nature Conservancy.

Tucker, C. J. (1979). Red and photographic infrared linear combinations for monitoring vegetation. *Remote Sensing of Environment*, *8*, 127–150.

Ustin, S. L., & Moser, T. J. (2002). Application of hyperspectral techniques to monitoring and management of invasive weed infestations. *Annual report to Strategic Environmental Research and Development Program (SERDP)*. Davis, CA: University of California (Unpublished report).

Ustin, S. L., Smith, M. O., Jacquemoud, S., Verstraete, M., & Govaerts, Y. (1999). Geobotany: Vegetation mapping for earth sciences. In A. N. Rencz (Ed.), *Remote sensing for the earth sciences: Manual of remote sensing*, *vol. 3* (3rd ed., pp. 189–248). New York: Wiley.

Weigand, C. L., & Richardson, A. J. (1987). Spectral components analysis: Rationale, and results for three crops. *International Journal of Remote Sensing*, *8*, 1011–1032.

Zarco-Tejada, P., & Miller, J. R. (1999). Land cover mapping at BOREAS using red edge spectral parameters from CASI imagery. *Journal of Geophysical Research*, *104*(D22), 921–933.

Zedler, P. H., & Scheid, G. A. (1988). Invasion of *Carpobrotus edulis* and *Salix lasiolepis* after fire in a coastal chaparral site in Santa Barbara county, California. *Madrono*, *35*(3), 196–201.